

Boosting CLIP Adaptation for Image Quality Assessment via Meta-Prompt Learning and Gradient Regularization

Xudong Li¹, Zihao Huang², Runze Hu², Yan Zhang¹, Liujuan Cao¹, Rongrong Ji¹

¹Key Laboratory of Multimedia Trusted Perception and Efficient Computing,
Ministry of Education of China, Xiamen University

lxd761050753@gmail.com, {bzhy986, caoliujuan, rrji}@xmu.edu.cn

²School of Information and Electronics, Beijing Institute of Technology
zzhowe1207@163.com, hrzlpk2015@gmail.com

Abstract

Image Quality Assessment (IQA) remains an unresolved challenge in the field of computer vision, due to complex distortion conditions, diverse image content, and limited data availability. The existing Blind IQA (BIQA) methods heavily rely on extensive human annotations to train models, which is both labor-intensive and costly due to the demanding nature of creating IQA datasets. To mitigate the dependence on labeled samples, this paper introduces a novel Gradient-Regulated Meta-Prompt IQA Framework (GRMP-IQA). This framework aims to fast adapt the powerful visual-language pre-trained model, CLIP, to downstream IQA tasks, significantly improving accuracy in scenarios with limited data. Specifically, the GRMP-IQA comprises two key modules: Meta-Prompt Pre-training Module and Quality-Aware Gradient Regularization. The Meta Prompt Pre-training Module leverages a meta-learning paradigm to pre-train soft prompts with shared meta-knowledge across different distortions, enabling rapid adaptation to various IQA tasks. On the other hand, the Quality-Aware Gradient Regularization is designed to adjust the update gradients during fine-tuning, focusing the model’s attention on quality-relevant features and preventing overfitting to semantic information. Extensive experiments on five standard BIQA datasets demonstrate the superior performance to the state-of-the-art BIQA methods under limited data setting, i.e., achieving SRCC values of 0.836 ($\uparrow 7.6\%$ vs. 0.760 on LIVEC) and 0.853 ($\uparrow 4.1\%$ vs. 0.812 on KonIQ). Notably, utilizing just **20%** of the training data, our GRMP-IQA outperforms most existing fully supervised BIQA methods.

1 Introduction

With the onset of the mobile internet era, the focus on computer vision has transitioned from initial concerns with compression and image processing (Sheikh, Sabir, and Bovik 2006) to handling user-generated content like smartphone photos and videos (Tu et al. 2021), and lately to AI-generated content (Li et al. 2023a). This progression has precipitated a marked escalation in the need for effective Blind Image Quality Assessment (BIQA) techniques, underscoring the importance of developing methodologies that can adeptly evaluate image quality without reference images.

Data-driven BIQA models (Song et al. 2023; Yang et al. 2022) based on deep neural networks have made signifi-

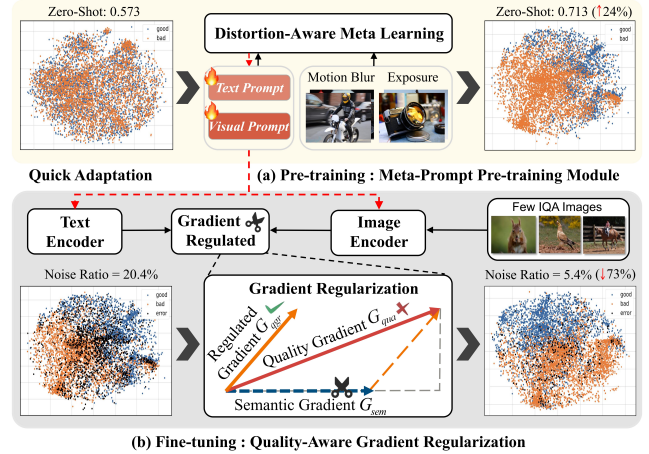


Figure 1: Intuitive diagram of GRMP-IQA. (a) demonstrates using meta-learning for efficient soft prompt initialization with quality prior that enhances zero-shot generalization ($\uparrow 24\%$), enabling the CLIP to adapt to BIQA tasks effectively. (b) shows a gradient regularization that fine-tunes the model by regularizing between quality and semantic gradients for IQA tasks, reducing the model’s overemphasis on semantic features. The black dots in t-SNE visualization represent noise samples with high semantic confidence (confidence > 0.8) but incorrect quality predictions. The noticeable decrease ($\downarrow 73\%$) in black dots indicates a reduction in semantic noise interference with quality assessments.

cant progress in recent years. However, the quality scores for distorted images are often measured using the Mean Opinion Score (MOS), which is the average of multiple ratings (sometimes up to 120). As a result, acquiring a sufficient number of IQA training samples is quite labor-intensive and cost-expensive. Recent BIQA approaches have tackled this challenge by leveraging the rich representations of large-scale datasets. Studies like (Qin et al. 2023; Xu et al. 2024) employ transfer learning by pretraining a model on ImageNet (Deng et al. 2009). Some works (Saha, Mishra, and Bovik 2023; Zhao et al. 2023; Srinath et al. 2024) propose IQA-specific pretext tasks, assuming that image distortions directly affect quality. These methods aim to extract quality representations efficiently through self-supervised learning, using scalable datasets. However, they often require exten-

sive pre-training and involve large-scale networks with millions of parameters, leading to high computational costs.

Recently, the pre-trained vision-language model CLIP (Radford et al. 2021) has achieved notable success in various downstream tasks. CLIP-IQA (Wang, Chan, and Loy 2023) shows promising zero-shot generalization in IQA tasks by using simple handcrafted prompts (e.g., “a good photo”). However, slight changes in these prompts can significantly impact performance, requiring experts to spend time on extensive validation. To overcome this, recent methods (Zhou et al. 2022b; Zhu et al. 2023; Jia et al. 2022) propose learning soft prompts (continuous embeddings) from small amounts of labeled data, offering a promising alternative to manual prompt design.

Despite the clear improvements in downstream task performance, prompt tuning for small labeled data generalization in IQA still faces two major limitations: (1) **Sensitivity to Initialization:** The performance of soft prompts is highly dependent on their initial settings, especially when training samples are limited. As shown in Fig. 2, there is a significant variation in the average SRCC performance across different initializations, necessitating careful tuning for each new IQA scenario, thereby limiting rapid adaptation. (2) **Reduced Generalization:** The CLIP encoder is designed for semantic content (e.g., identifying cats or dogs) rather than image quality attributes (e.g., noise or sharpness). When fine-tuned with a small sample size, the model tends to overfit to spurious correlations (such as semantic noise) rather than true image quality. As illustrated in Fig. 1, when the CLIP encoder is fine-tuned on a limited dataset, the latent space contains many instances (black dots) that confidently and accurately predict image semantics (with confidence levels above 0.8) but fail to correctly assess image quality.

To address these limitations, we propose the Gradient-Regulated Meta-Prompt learning for IQA (GRMP-IQA), which operates in two main stages: (1) Meta Prompt Pre-training and (2) Quality-Aware Gradient Regularization. In the first stage, we refine the initialization of soft prompts to reduce their sensitivity and improve adaptability to new IQA scenarios. We design meta-training tasks using a well-annotated dataset with various distortions (e.g., overexposure, blur) and employ a bi-level gradient descent method. This allows the model to generalize across different IQA tasks by learning shared meta-knowledge of quality across distortions. In the second stage, the QGR module modulates gradient updates during fine-tuning by balancing the similarity between quality knowledge direction G_{qua} and semantic knowledge direction G_{sem} . By clipping the quality gradient G_{qua} along the semantic gradient G_{sem} , the module reduces reliance on semantic content, thereby enhancing the accuracy of image quality assessments. Moreover, fine-tuning only CLIP’s text branch can misalign quality perception between the image and text branches, limiting generalization (Khattak et al. 2023a). To resolve this, we integrate text prompt tuning (CoOp (Zhou et al. 2022b)) and visual prompt tuning (VPT (Jia et al. 2022)) by jointly meta-learning initializations for both, ensuring complementary optimization to better adapt CLIP to new IQA scenarios (Tab. 4).

Our contributions can be summarized as follows:

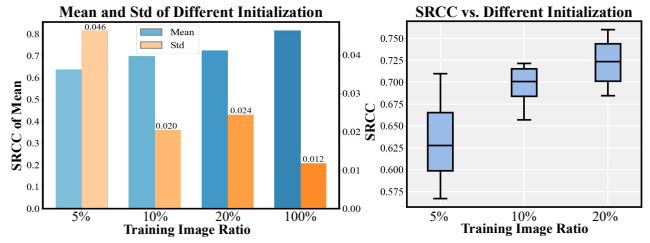


Figure 2: The fine-tuning results on the LIVEC dataset using CoOp (Zhou et al. 2022b) demonstrate that the accuracy of prompt tuning is significantly influenced by the initial random initialization of the prompt. This effect becomes more evident with limited training data, emphasizing the importance of prompt initialization under data constraints.

- We propose a Meta Prompt Pre-training method that organizes meta tasks based on image distortion types and optimizes soft textual and visual prompts to gain shared quality meta-knowledge, enabling CLIP to rapidly adapt across various IQA scenarios.
- We develop a novel Quality-Aware Gradient Regularization method that clips gradients aligned with semantic directions to balance semantic and quality information during fine-tuning, ensuring the model prioritizes image quality while still integrating relevant semantic context.
- Extensive empirical evidence underscores the effectiveness and efficiency of our approach. Remarkably, with only 200 data samples, our method surpasses SOTA models on the LIVEC dataset (using 20% of the training data) and achieves highly competitive performance on the KonIQ dataset (using 2% of the training data).

2 Related Work

2.1 Deep Learning Based BIQA methods

Early CNN-based methods utilized standard pre-training and fine-tuning pipelines (Zhang et al. 2018; He et al. 2016), while meta-learning approaches like MetaIQA (Zhu et al. 2020) improved adaptability from synthetic to real-world images. However, CNNs struggle with non-local features, a gap filled by ViT-based approaches (Golestaneh, Dadsetan, and Kitani 2022; Ke et al. 2021). Recent models like LIQE (Zhang et al. 2023) integrate CLIP’s multi-task learning capabilities, enhancing IQA with supervised fine-tuning across datasets. Yet, these methods heavily rely on extensive annotated data, posing significant cost and time challenges. In contrast, limited-data BIQA models remain under-explored. DEIQT (Qin et al. 2023) shows that fine-tuning a pre-trained ViT model can yield good results with less annotation, though improvement is still needed. Self-supervised methods (Saha, Mishra, and Bovik 2023; Zhao et al. 2023; Srinath et al. 2024) attempt to address data limitations by devising pre-training tasks aligned with BIQA. However, they require large pretext datasets and extensive training, leading to high costs. In contrast, our approach uses prompt tuning to significantly reduce pre-training expenses. By leveraging the synergy between pre-trained CLIP model insights and IQA

specifics during fine-tuning, our model is poised to outperform fully supervised BIQA with minimal data.

2.2 Prompt Tuning

Inspired by Natural Language Processing, recent research has adapted vision-language pre-trained models to downstream tasks by learning task-specific prompts in an end-to-end manner (Wu and Shi 2022; Vu et al. 2021). Given the limited labeled data during training, prompt tuning is often treated as a few-shot learning task (Fu, Fu, and Jiang 2021; Zhang et al. 2024; Li et al. 2023b). CoOp (Zhou et al. 2022b) optimizes prompt vectors in the CLIP language branch for task adaptation, though it struggles with generalization to novel tasks. To address this, CoCoOp (Zhou et al. 2022a) uses a lightweight meta-network to generate input-conditioned tokens, improving adaptability. Kg-CoOp (Yao, Zhang, and Xu 2023) further enhances generalization by narrowing the gap between handcrafted and learnable prompts. While these methods focus on textual prompts, significant work has also explored visual prompts for task adaptation (Jia et al. 2022). By incorporating trainable prompts into both the language and visual branches of CLIP, methods like MaPLe (Khattak et al. 2023a) and PromptSRC (Khattak et al. 2023b) achieve substantial performance improvements across base and novel tasks.

3 Methodology

3.1 Overview

In this paper, we introduce the *Gradient-Regulated Meta-Prompt Image Quality Assessment* (GRMP-IQA), which aims to adapt the CLIP for BIQA tasks with a few training samples. As depicted in Fig. 3, GRMP-IQA consists of two primary module: the *Meta-Prompt Pre-training Module* (MPP) and the *Quality-Aware Gradient Regularization* (QGR). The MPP module pre-trains visual-text prompts to acquire shared meta-knowledge on distortions, enabling quick adaptation to various IQA scenarios. The QGR module plays a key role in fine-tuning by adjusting gradient updates to prevent overfitting to semantic content.

Pre-training stage (Sec. 3.3). We randomly sample a mini-batch from distortion meta-tasks, partitioning it into a support set $\mathcal{D}^{\text{support}}$ and a query set $\mathcal{D}^{\text{query}}$. A bi-level gradient descent method progresses from the Inner-Loop on $\mathcal{D}^{\text{support}}$ to the Outer-Loop on $\mathcal{D}^{\text{query}}$ to optimize the learnable visual-textual prompts $[\theta_T, \theta_V]$. These prompts are then used as initial conditions for fine-tuning.

Fine-tuning stage (Sec. 3.4). Given an input image x and a semantic prompt w_i =“a photo of a [class].”, we predict the class probability distribution $p^{\text{sem}}(w_i|x)$ and $p^{\text{qua}}(w_i|x)$ of image x using both the origin semantic CLIP model and fine-tuned CLIP model and compute the gradient of the KL divergence loss $\nabla \mathcal{L}_{kl}$ as a measure of general semantic direction. Simultaneously, according to prompt θ_T and image x , we compute the gradient $\nabla \mathcal{L}_{ce}$ of the quality loss between the predicted quality and the actual quality label as the quality direction. Finally, we refine the IQA task direction $G_{\text{qua}} \rightarrow G_{\text{qgr}}$ by clipping gradients aligned with the general semantic direction G_{sem} . This

approach ensures that the model prioritizes image quality, thereby minimizing the impact of semantic noise.

3.2 Visual-Text Meta-Prompt

Visual Meta-Prompt. We use Deep Prompt Tuning (DPT (Zhou et al. 2022b)) as our Visual Meta-Prompt. The input embedding for the l layer’s self-attention module in the ViT-based image encoder is denoted as $\{f^l, h_1^l, h_2^l, \dots, h_N^l\}$, where f^l represents the classification (CLS) token, and H^l denotes the image patch embeddings. A learnable token P^l is appended to the token sequence in each ViT layer, and the Multi-Head Attention module (MHA) processes the tokens as:

$$[f^l, -, H^l] = \text{Layer}^l([f^{l-1}, P^{l-1}, H^{l-1}]), \quad (1)$$

where the output of P^l is discarded and not passed to the next layer, serving only as a set of learnable parameters.

Text Meta-Prompt. We define the quality prompt as containing $q_i = \{v_1, v_2, \dots, v_M, [\text{quality}]\}$, where q_i denotes the learnable text feature for the i -th class, and the length of vector M is set to 4 in our GRMP-IQA. We introduce two categories of embedding quality markers and $[\text{quality}] \in \{\text{“high quality”}, \text{“low quality”}\}$.

3.3 Meta-Prompt Pre-training Module

During meta-learning, we optimize the learnable visual-text prompt $\theta = [\theta_T, \theta_V]$. For an input image x , the textual encoder $g(\cdot)$ processes the quality prompts q_i , while the visual encoder extracts the feature vector f . The probability of predicting high quality is:

$$p(q_{\text{high}}|x) = \frac{\exp(\langle g(q_{\text{high}}), f \rangle / \tau)}{\exp(\langle g(q_{\text{high}}), f \rangle / \tau) + \exp(\langle g(q_{\text{low}}), f \rangle / \tau)}, \quad (2)$$

where q_{high} and q_{low} donate high quality and low quality category prompt, $p(q_{\text{high}}|x)$ represents the estimated probability that the quality of image x is “high quality”, τ is a temperature parameter learned by CLIP, and $\langle \cdot, \cdot \rangle$ denotes cosine similarity. The labeled quality scores are then rescaled to 0-1, denoted as y , and the loss function is calculated as:

$$\mathcal{L} = -(y \log(p(q_{\text{high}}|x)) + (1-y) \log(1-p(q_{\text{high}}|x))). \quad (3)$$

Constructing Distortion Meta-Knowledge Task. As noted by (Ma et al. 2019; Zhu et al. 2020), the ability to detect various types of image distortions is crucial for developing BIQA models with strong generalization capabilities across diverse scenarios. Moreover, the efficacy of prompt tuning is significantly dependent on the initial configuration of the prompts. This initial setup greatly affects the CLIP vision-language model’s ability to swiftly adapt to different IQA scenarios. Drawing inspiration from the “learn to learn” ethos inherent in the deep meta-learning paradigm (Vanschoren 2018; Zhu et al. 2020), we propose an optimization-based method for effectively pre-training visual-text prompts. These prompts incorporate shared quality insights from various image distortions, thereby enhancing CLIP’s swift adaptability to IQA tasks. To investigate the general rules of image distortion, we first constructed a K_t -way task-specific BIQA task, denoted as \mathcal{T}_t .

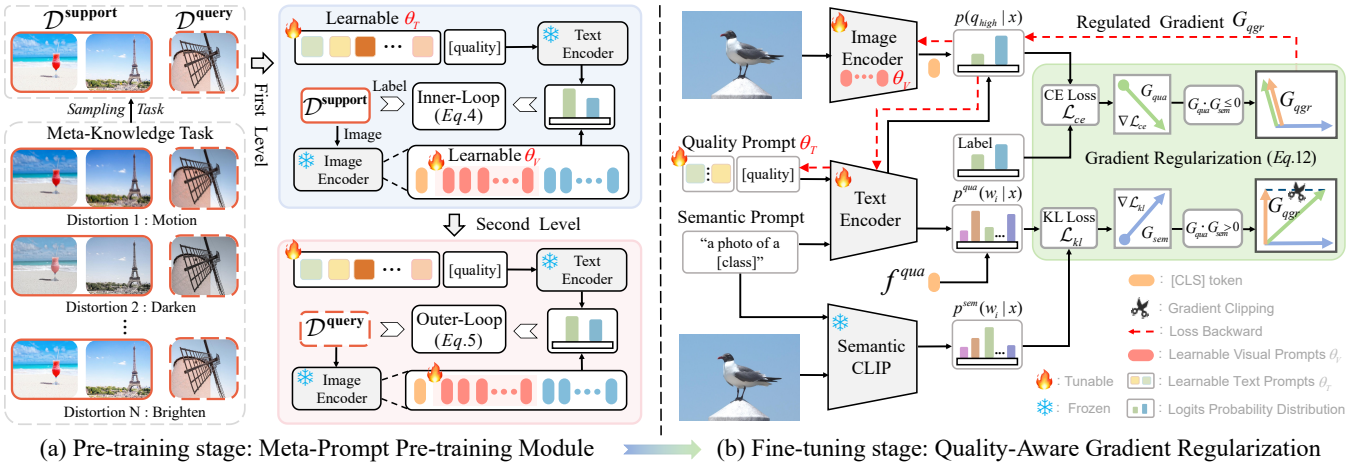


Figure 3: The overview of our GRMP-IQA. The core modules are the Meta-Prompt Pre-training and Quality-Aware Gradient Regularization, corresponding to two training processes. At the pre-training stage, we establish a distortion Meta-Knowledge task for BIQA tasks, and the bi-level gradient descent is utilized to train visual-text meta-prompt $[\theta_T, \theta_V]$ (Sec. 3.3). These optimized prompts then serve as initial settings to efficiently adapt the CLIP model to IQA tasks with limited labels. At the fine-tuning stage, we adjust IQA task gradients G_{qua} by clipping gradients aligned with semantic task gradients G_{sem} to generate G_{qgr} for backward updates (Sec. 3.4), thereby mitigating the influence of semantic noise on quality predictions.

Then, it is used to build the meta-training set as $\mathcal{D}^{meta} = \{\mathcal{D}_{\mathcal{T}_t}^{support}, \mathcal{D}_{\mathcal{T}_t}^{query}\}_{t=1}^T$. Here, $\mathcal{D}_{\mathcal{T}_t}^{support}$ and $\mathcal{D}_{\mathcal{T}_t}^{query}$ represent the support and query sets for each task, respectively, with T representing the total number of tasks. To simulate the process of prompt generalization to different distortions in BIQA scenarios, we randomly sample k tasks as a mini-batch from the meta-training set, where $1 \leq k \leq T$, to perform bi-level gradient optimization.

Distortion-Aware Meta-prompt Learning. Our approach employs a bi-level gradient descent technique to bridge the learning process from the support to the query set. Specifically, it mainly consists of two optimization steps. In the Inner-Loop (the first level), we compute the gradients of the prompt parameters using the support set and apply the first update. In the Outer-Loop (the second level), we assess the performance of the updated model on the query set. This bi-level structure enables the prompt to rapidly acquire generalization ability across diverse BIQA contexts by optimizing meta-prompts to acquire shared quality prior knowledge.

Inner-Loop. The objective of the Inner-Loop stage is to adapt the meta-prompt, denoted by $\theta = [\theta_T, \theta_V]$, to the t^{th} support set $\mathcal{D}_{\mathcal{T}_t}^{support}$ within the mini-batch. During the first level of updates, we determine the loss $\mathcal{L}(\theta, \mathcal{D}_{\mathcal{T}_t}^{support})$, following which the model parameters are updated on the support set using the inner learning rate α , as specified by:

$$\theta'_i \leftarrow \theta - \alpha \nabla \theta \mathcal{L}(\theta, \mathcal{D}_{\mathcal{T}_t}^{support}), \quad (4)$$

Outer-Loop. In a similar vein, the second level of updates adjusts the parameters θ'_i based on the query set $\mathcal{D}_{\mathcal{T}_t}^{query}$:

$$\theta_i \leftarrow \theta'_i - \alpha \nabla \theta \mathcal{L}(\theta, \mathcal{D}_{\mathcal{T}_t}^{query}). \quad (5)$$

The culmination of this process for a mini-batch of meta-tasks involves the aggregation of gradients from all tasks to

update the final model parameters, following the update rule:

$$\theta \leftarrow \theta - \beta \frac{1}{k} \sum_{i=1}^k (\theta - \theta_i), \quad (6)$$

where β represents the outer learning rate. Meta-learning effectively trains the learnable prompts $\theta = [\theta_T, \theta_V]$, ensuring their generalization across various image distortions.

3.4 Quality-Aware Gradient Regularization

We denote the original semantic CLIP model as V^{sem} , and the CLIP model obtained from the Meta-Prompt Pre-training Module as V^{qua} . Recent studies (Zhao et al. 2023) have shown that IQA tasks can be misaligned with the high-level semantic representations of upstream tasks, leading to overfitting and reduced generalization. To mitigate this issue, we introduce Quality-aware Gradient Regularization (QGR), which uses directional guidance from the original CLIP model’s semantic predictions V^{sem} to refine quality gradient updates during fine-tuning on IQA tasks. This approach aims to reduce the focus on semantics and enhance the model’s ability to evaluate image quality effectively.

Specifically, to derive a general semantic direction G_{sem} , we first design a hard prompt following (Ying et al. 2020): $w_i = \text{“a photo of a [class]”}$ representing one of nine categories: “animal”, “cityscape”, “human”, “indoor”, “landscape”, “night”, “plant”, “still-life”, “others”. This prompt w_i is input into the text encoders of V^{sem} and V^{qua} , generating text features that align with image features from their respective visual encoders. This results in zero-shot semantic prediction probabilities $p^{sem}(w_i|x)$ and $p^{qua}(w_i|x)$. To avoid overemphasis on semantics in V^{qua} , we measure the semantic attention by calculating the KL divergence be-

Method	LIVEC			KonIQ			CSIQ			LIVE			PIPAL		
	50	100	200	50	100	200	50	100	200	50	100	200	50	100	200
HyperIQA (Su et al. 2020)	0.648	0.725	0.790	0.615	0.710	0.776	0.790	0.824	0.909	0.892	0.912	0.929	0.102	0.302	0.379
MetalQA (Zhu et al. 2020)	0.604	0.626	0.669	0.618	0.620	0.660	0.784	0.849	0.894	0.840	0.880	0.919	0.332	0.348	0.371
DEIQT (Qin et al. 2023)	0.667	0.718	0.812	0.638	0.682	0.754	0.821	0.891	0.941	0.920	0.942	0.955	<u>0.396</u>	0.410	0.436
MANIQA (Yang et al. 2022)	0.642	0.769	0.797	0.652	0.755	0.810	0.794	0.847	0.874	0.909	0.928	0.957	0.136	0.361	0.470
CONTRIQUE (Madhusudana et al. 2022)	0.695	0.729	0.761	0.733	0.794	0.821	0.840	0.926	0.940	0.891	0.922	0.943	0.379	0.437	0.488
Re-IQA (Saha, Mishra, and Bovik 2023)	0.591	0.621	0.701	0.685	0.723	0.754	<u>0.893</u>	0.907	0.923	0.884	0.894	0.929	0.280	0.350	0.431
CLIP (Radford et al. 2021)	0.664	0.721	0.733	0.736	0.770	0.782	0.841	0.892	0.941	0.896	0.923	0.941	0.254	0.303	0.368
CLIP-IQA (Wang, Chan, and Loy 2023)	0.695	0.738	0.746	0.692	0.743	0.762	-	-	-	-	-	-	-	-	-
LIQE (Zhang et al. 2023)	0.691	0.769	0.810	0.759	0.801	0.832	0.838	0.891	0.924	0.904	0.934	0.948	-	-	-
GRepQ (Srinath et al. 2024)	<u>0.760</u>	<u>0.791</u>	<u>0.822</u>	<u>0.812</u>	<u>0.836</u>	<u>0.855</u>	0.878	0.914	<u>0.941</u>	<u>0.926</u>	<u>0.937</u>	<u>0.953</u>	0.390	<u>0.450</u>	<u>0.498</u>
GRMP-IQA (Ours)	0.836	0.857	0.875	0.853	0.872	0.883	0.893	<u>0.917</u>	0.941	0.932	0.943	0.968	0.474	0.512	0.546

Table 1: SRCC performance comparison of our method with other IQA methods trained on limited labels. Bold indicates the best results, underlined marks the second-best, and the fifth-to-last through second-to-last lines show the CLIP-based IQA.

tween $p^{sem}(w_i|x)$ and $p^{qua}(w_i|x)$:

$$\mathcal{L}_{kl}(V^{qua}) = - \sum_i p^{sem}(w_i|x) \log \frac{p^{qua}(w_i|x)}{p^{sem}(w_i|x)}. \quad (7)$$

Conversely, we obtain the quality optimization direction by calculating the cross-entropy $\mathcal{L}_{ce}(V^{qua})$ between the prediction $p(q_{high}|x)$ and the ground truth y , as shown in Eq. 3. We then balance the learning between quality and semantics by adjusting the gradients of the tasks within a shared representation space. The gradients $\nabla \mathcal{L}_{ce}(V^{qua})$ and $\nabla \mathcal{L}_{kl}(V^{qua})$ are represented as G_{qua} and G_{sem} , and the relationship between them can be described in two aspects:

(1) If the angle between G_{qua} and G_{sem} is less than 90 degrees, it indicates that the optimization directions for IQA quality knowledge and general semantic knowledge are consistent. In such cases, we clip the G_{qua} along its component G_{\parallel} that parallel to the semantic direction G_{sem} , to modulate the model’s original quality-aware optimization path, thereby preventing overfitting to semantic correlations.

(2) Conversely, if the angle between two areas of knowledge is more than 90 degrees, it means they are heading in different directions during improvement. In such situations, we don’t adjust the quality gradient G_{qua} , allowing the model to learn quality-aware features according to the original optimization direction. In conclusion, our gradient regularization strategy is mathematically formulated as:

$$G_{qgr} = \begin{cases} G_{qua} & \text{if } G_{qua} \cdot G_{sem} \leq 0, \\ G_{qua} - \lambda \frac{G_{qua} \cdot G_{sem}}{\|G_{sem}\|^2} G_{sem} & \text{otherwise,} \end{cases} \quad (8)$$

Here, λ is introduced to generalize the formulation, providing flexibility in controlling the influence of general knowledge. Specifically, $\lambda = 1$ projects G_{qua} onto the orthogonal direction of G_{sem} , while $\lambda = 0$ reduces QGR to CoOp.

4 Experiments

4.1 Datasets and Evaluation Protocols

We conduct experiments on seven typical BIQA datasets and one AI-generated dataset, AGIQA-3K (Li et al. 2023a) (results in the supplementary materials). The seven typical datasets include LIVEC (Ghadiyaram and Bovik 2015), KonIQ (Hosu et al. 2020), LIVEFB (Ying et al. 2020),

and SPAQ (Fang et al. 2020), which feature authentic distortions, and PIPAL (Jinjin et al. 2020), LIVE (Sheikh, Sabir, and Bovik 2006), and CSIQ (Larson and Chandler 2010), which feature synthetic distortions. LIVEC contains 1,162 mobile device images, SPAQ includes 11,125 photos from 66 smartphones, KonIQ has 10,073 images from open sources, and LIVEFB is the largest real-world dataset with 39,810 images. For synthetic distortions, LIVE and CSIQ contain 779 and 866 images with 5 and 6 types of distortions, respectively. PIPAL, a challenging dataset, includes 23,200 images with 40 types of distortions, including GAN-generated artifacts. We use Spearman’s Rank Correlation Coefficient (SRCC) and the Pearson Linear Correlation Coefficient (PLCC) outcomes as metrics to quantify the monotonousness and accuracy of predictions.

4.2 Implementation Details and Setups

We build our model on CLIP-B/16 (Radford et al. 2021). During pre-training, we optimize the visual-text prompt, while in fine-tuning, we adjust the last four blocks of the image and text encoders. For competing models, we use either public implementations or re-train them on our datasets. We use 80% of each dataset for training and 20% for testing. To ensure content independence in datasets with synthetic distortions, training and testing sets are split by reference images. For more details, please refer to the Appendix.

Meta Pre-training Stage. We pre-train on TID2013 (Ponomarenko et al. 2015) and KADID-10K (Lin, Hosu, and Saupé 2019), which contain extensive distortion information. We set the learning rates α and β to 1e-4 and 1e-2, and train for 50 epochs using Adam (Kingma and Ba 2014).

Fully Supervised Setting. For fully supervised training, we randomly crop each input image into 10 patches of 224×224 resolution and train the model for 9 epochs using AdamW (Loshchilov and Hutter 2019). The learning rate is 5×10^{-6} , with a scheduler over 9 decay epochs. The batch size is 16 for LIVEC and 128 for KonIQ.

Few-Shot Learning Setting. In the few-shot setting, we train GRMP-IQA with 50, 100, or 200 samples from 80% of the training images, following the CoOp (Zhou et al. 2022b) schedule. The λ parameter is set to 5.

Method	LIVE		CSIQ		LIVEC		KonIQ		LIVEFB		SPAQ	
	PLCC	SRCC	PLCC	SRCC	PLCC	SRCC	PLCC	SRCC	PLCC	SRCC	PLCC	SRCC
Training Ratio	20%	20%	20%	20%	20%	20%	30%	30%	10%	10%	20%	20%
DEIQT (Qin et al. 2023)	0.968	0.965	0.885	0.862	0.822	0.792	0.922	0.903	0.624	0.538	0.912	0.908
GRMP-IQA (Ours)	0.972	0.970	0.958	0.951	0.897	0.875	0.936	0.925	0.686	0.604	0.925	0.920
Training Ratio	80%	80%	80%	80%	80%	80%	80%	80%	80%	80%	80%	80%
MetalQA (Zhu et al. 2020)	0.959	0.960	0.908	0.899	0.802	0.835	0.856	0.887	0.507	0.540	-	-
CONTRIQUE (Madhusudana et al. 2022)	0.961	0.960	0.955	0.942	0.857	0.845	0.906	0.894	0.641	0.580	0.919	0.914
DEIQT (Qin et al. 2023)	0.982	0.980	0.963	0.946	0.894	0.875	0.934	0.921	0.663	0.571	0.923	0.919
Re-IQA (Saha, Mishra, and Bovik 2023)	0.971	0.970	0.960	0.947	0.854	0.840	0.923	0.914	0.733	0.645	0.925	0.918
LIQE (Zhang et al. 2023)	0.951	0.970	0.939	0.936	0.910	0.904	0.908	0.919	-	-	-	-
CLIP-IQA+ (Wang, Chan, and Loy 2023)	-	-	-	-	0.832	0.805	0.909	0.895	0.593	0.575	0.866	0.864
QFM-IQM (Li et al. 2024)	0.983	0.981	0.965	0.954	0.913	0.891	0.936	0.922	0.667	0.567	0.924	0.920
LoDa (Xu et al. 2024)	0.979	0.975	-	-	0.899	0.876	0.944	0.932	0.679	0.578	0.928	0.925
GRMP-IQA (Ours)	0.983	0.981	0.974	0.968	0.916	0.897	0.945	0.934	0.704	0.616	0.932	0.927

Table 2: Performance comparison measured by medians of SRCC and PLCC, and **bold** entries indicate the top two results.

Training	LIVEFB		LIVEC		KonIQ		LIVE		CSIQ	
Testing	KonIQ	LIVEC	KonIQ	LIVEC	CSIQ	LIVE	CSIQ	LIVE	CSIQ	LIVE
DBCNN	0.716	0.724	0.754	0.755	0.758	0.877				
HyperIQA	0.758	0.735	0.772	0.785	0.744	0.926				
TReS	0.713	0.740	0.733	0.786	0.761	-				
DEIQT	0.733	0.781	0.744	0.794	0.781	0.932				
CLIP-IQA+	0.631	0.620	0.697	0.803	-	-				
LoDa	0.763	0.805	0.745	0.811	-	-				
GRMP-IQA	0.765	0.790	0.782	0.831	0.809	0.935				

Table 3: SRCC on the cross datasets validation. The best performances are highlighted in boldface.

4.3 Few-Shot Performance Comparison

The GRMP-IQA model acquires a substantial amount of image assessment knowledge, allowing it to furnish powerful and rich priors for various IQA scenarios. Consequently, our model can achieve excellent evaluation performance with a relatively small amount of data. Specifically, we randomly select subsets of 50, 100, and 200 samples from the training set for training and evaluate the same test data as the full data supervised learning. We report the median performance obtained across 10 splits. Tab. 1 presents the comparison results in this few-shot setting. It can be observed that our method outperforms the second-best model GRepQ (Srinath et al. 2024) by a significant margin, even though GRepQ is specifically designed for few-shot learning. Furthermore, our approach significantly outperforms MetalQA, a meta-learning-based method, highlighting the superiority of meta-prompts for rapid adaptation of CLIP to various IQA scenarios. These results clearly demonstrate the strong capability of our method to learn image quality even with limited labels. For comparison, we also present results in the fully-supervised setting in Table 2 as an extreme case.

4.4 Performance comparison with SOTA

The results of the comparison between GRMP-IQA and other BIQA methods, which include self-training BIQA

methods like CONTRIQUE (Madhusudana et al. 2022) and Re-IQA (Saha, Mishra, and Bovik 2023), as well as CLIP-based BIQA methods such as LIQE (Zhang et al. 2023) and CLIP-IQA+ (Wang, Chan, and Loy 2023), are presented in Tab. 2. It can be observed on six of the eight datasets that GRMP-IQA outperforms all other methods in terms of performance. Achieving leading performance on all of these datasets is a challenging task due to the wide range of image content and distortion types. Therefore, these observations confirm the effectiveness and superiority of GRMP-IQA in accurately characterizing image quality. Notably, our method achieved results competitive with SOTA methods by utilizing just 20% of the training data from the training set.

4.5 Generalization Capability Validation

To assess the generalization capacity of GRMP-IQA, we conducted cross-dataset validation experiments. In these experiments, the model was trained on one dataset (after meta-learning) and subsequently tested on others, without any adjustment of parameters. The outcomes of these experiments are displayed in Tab. 3, which shows the SRCC achieved across five different datasets. Notably, GRMP-IQA outperforms state-of-the-art (SOTA) models in all six experiments involving cross-authentic datasets. This includes significant performance enhancements in the LIVEC and KonIQ datasets. Moreover, GRMP-IQA exhibits strong competitiveness on synthetic datasets such as LIVE and CSIQ.

4.6 Ablation Study

Effect of Meta-Prompt Pre-training Module. This module consists of three key components: meta-learning, text meta-prompts, and visual meta-prompts. In Tab. 4, we perform ablation studies to evaluate the zero-shot capabilities of these components across various datasets. The baseline uses a CLIP model pre-trained on classification tasks. The second row shows meta-learning without prompts, fine-tuning CLIP’s visual and text encoders. The third and fourth rows focus on fine-tuning only the text or visual prompts, respectively, during meta-learning. The fifth row presents prompt tuning without meta-learning. Specifically, the second row

Components			LIVEC		KonIQ		PIPAL	
Meta	Text	Visual	PLCC	SRCC	PLCC	SRCC	PLCC	SRCC
			0.579	0.598	0.592	0.573	0.216	0.203
✓			0.639	0.589	0.556	0.554	0.367	0.371
✓	✓		0.699	0.689	0.679	0.609	0.323	0.312
✓		✓	0.776	0.742	0.736	0.701	0.357	0.369
		✓	0.759	0.709	0.622	0.592	0.362	0.396
✓	✓	✓	0.808	0.770	0.744	0.713	0.410	0.434

Table 4: Ablation experiments with Meta-Prompt Pre-training component under zero-shot on three datasets. The best performances are highlighted in boldface.

Component		LIVEC		KonIQ	
Pre-training	Meta-learning	PLCC	SRCC	PLCC	SRCC
		0.825	0.796	0.788	0.764
✓		0.823	0.788	0.792	0.761
✓	✓	0.858	0.828	0.844	0.811

Table 5: Ablation study on meta-learning effectiveness, showing fine-tuning results on LIVEC with 50 samples.

reveals that meta-learning allows CLIP to learn shared quality knowledge across different distortions, improving IQA performance. However, adjusting CLIP’s weights reduces its original generalization, leading to lower performance on KonIQ. The third and fourth rows show that fine-tuning only the text or visual prompts significantly enhances zero-shot testing, especially on real-world datasets like KonIQ and LIVEC, by preserving CLIP’s generalization. The best results occur when both prompts are used together, confirming their mutual benefit. Finally, comparing the last row with the fifth shows that without meta-learning, prompt tuning leads to overfitting and reduced generalization.

Effect of Meta-learning. To further investigate whether the effectiveness of our method derives from meta-learning, we conducted an ablation study. Specifically, as shown in rows 1 and 2 of Tab. 5, when using Empirical Risk Minimization without meta-learning pre-training on two synthetic dataset, the fine-tuning performance on LIVEC and KonIQ dataset was even worse than the baseline without pre-training. This indicates that additional pre-training data does not necessarily enhance performance and may even lead to overfitting. In contrast, the proposed meta-learning strategy allows the model to effectively leverage the generalizable quality priors obtained from the available external data, leading to significant performance improvements across different datasets.

Effect of Gradient Regularization. We performed ablation studies on the Quality-Aware Gradient Regularization (QGR) module. As shown in Tab. 6 and Fig. 4(a), without QGR, especially with very limited training data (e.g., 50 images), the model is prone to overfitting, leading to a sharp drop in generalization performance. QGR, by modulating training gradients, effectively reduces this overfitting and significantly improves adaptability to the test dataset.

Method	Labels	50		100	
	Dataset	PLCC	SRCC	PLCC	SRCC
w/o QGR	LIVEC	0.858	0.828	0.875	0.848
w/ QGR	LIVEC	0.864	0.836	0.883	0.857
w/o QGR	KonIQ	0.844	0.811	0.872	0.840
w/ QGR	KonIQ	0.880	0.853	0.896	0.872

Table 6: Ablation experiments with QGR in few-shot setting. The best performances are highlighted in boldface.

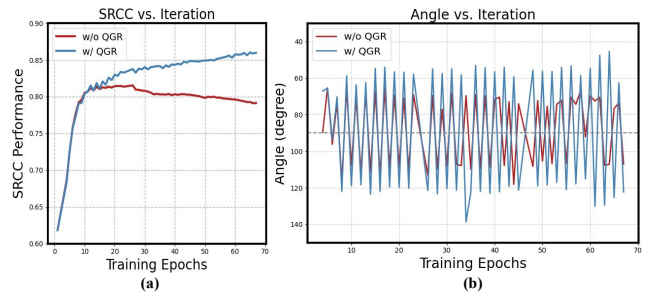


Figure 4: (a) SRCC value during training. (b) Angles between G_{qua} and G_{sem} during training on KonIQ dataset. Under the constraints of QGR, our GRMP-IQA effectively captures the correlation between downstream quality knowledge and upstream general semantic knowledge.

To illustrate QGR’s impact, we analyzed the angular difference between gradients G_{qua} and G_{sem} during training, as shown in Fig. 4(b). Without QGR, the angle between G_{qua} and G_{sem} tends toward 90 degrees, reflecting orthogonality typical of high-dimensional random vectors (Cai, Fan, and Jiang 2013). In contrast, QGR fosters a correlation between quality and semantic directions, improving the model’s ability to process quality-related information and reducing overfitting in limited datasets.

Effect of soft weight λ . As detailed in Tab. 7, a small λ weakens QGR’s effectiveness, while a large λ causes significant gradient changes and reduces performance. Based on this trade-off, we adopt $\lambda = 5$ in our experiments.

5 Qualitative Analysis

To further assess our framework’s generalization, we trained models on the entire LIVE database and then tested them using the gMAD competition (Ma et al. 2016b) on the Waterloo Database (Ma et al. 2016a). gMAD efficiently selects image pairs with maximum quality difference predicted by an attacking IQA model to challenge another defending model which considers them to be of the same level of quality. The selected pairs are shown to the observer to determine whether the attacker or the defender is robust. As shown in Fig. 5, In the first two columns, our model attacks the competing method DEIQT, where each column represents images chosen from the poorer and better quality levels predicted by the defender. In the last two columns, we fix our model as the defender, giving image pairs selected from

λ	50		100		200	
	PLCC	SRCC	PLCC	SRCC	PLCC	SRCC
1	0.850	0.812	0.874	0.839	0.893	0.866
3	0.864	0.839	0.890	0.865	0.903	0.878
5	0.880	0.853	0.896	0.872	0.908	0.883
7	0.876	0.851	0.895	0.870	0.905	0.881

Table 7: The ablation study about soft weight λ in Eq.8.

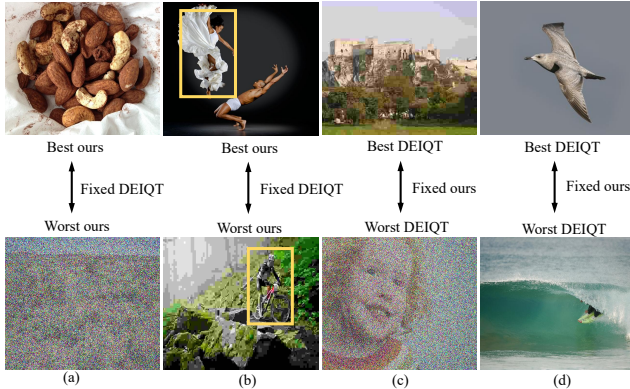


Figure 5: gMAD results between DEIQT (Qin et al. 2023) and ours. (a) Fixed DEIQT at low quality. (b) Fixed DEIQT at high quality. (c) Fixed ours at low quality. (d) Fixed ours at high quality.

poorer and better quality levels, respectively. From Fig. 5, it is evident that when our model serves as the defender, the image pairs chosen by the attacker show little perceptual quality change, whereas, as the attacker, our model selects image pairs with more significant quality differences in succession. This indicates that the model has strong defensive and offensive capabilities. Additionally, it is important to highlight that the image pairs in the second column, which share similar semantic information, misled the DEIQT into classifying them as similar quality. Conversely, our model effectively identified the quality differences between them. These findings further underscore the strong generalization capability of our model in tackling complex distortions in real-world images.

6 Conclusion

In this research, we introduce the Gradient-Regulated Meta-Prompt Image Quality Assessment (GRMP-IQA) framework, which excels in generalization with limited data samples. This framework features a meta-learned soft prompt initialization module that quickly adapts to specific IQA tasks using pre-trained meta-knowledge. Additionally, an adaptive gradient regulation module refines the gradient trajectory during fine-tuning, focusing updates on image quality assessment while minimizing the impact of semantic content. Comprehensive experiments on various BIQA datasets validate the superior generalization of our framework, especially in data-scarce scenarios.

References

- Cai, T.; Fan, J.; and Jiang, T. 2013. Distributions of angles in random packing on spheres. *The Journal of Machine Learning Research*, 14(1): 1837–1864.
- Deng, J.; Dong, W.; Socher, R.; Li, L.-J.; Li, K.; and Fei-Fei, L. 2009. Imagenet: A large-scale hierarchical image database. In *2009 IEEE conference on computer vision and pattern recognition*, 248–255. Ieee.
- Fang, Y.; Zhu, H.; Zeng, Y.; Ma, K.; and Wang, Z. 2020. Perceptual quality assessment of smartphone photography. In *Proceedings of the IEEE/CVF Conference on Computer Vision and Pattern Recognition*, 3677–3686.
- Fu, Y.; Fu, Y.; and Jiang, Y.-G. 2021. Meta-fdmixup: Cross-domain few-shot learning guided by labeled target data. In *Proceedings of the 29th ACM international conference on multimedia*, 5326–5334.
- Ghadiyaram, D.; and Bovik, A. C. 2015. Massive online crowdsourced study of subjective and objective picture quality. *IEEE Transactions on Image Processing*, 25(1): 372–387.
- Golestaneh, S. A.; Dadsetan, S.; and Kitani, K. M. 2022. No-reference image quality assessment via transformers, relative ranking, and self-consistency. In *Proceedings of the IEEE/CVF Winter Conference on Applications of Computer Vision*, 1220–1230.
- He, K.; Zhang, X.; Ren, S.; and Sun, J. 2016. Deep residual learning for image recognition. In *Proceedings of the IEEE conference on computer vision and pattern recognition*, 770–778.
- Hosu, V.; Lin, H.; Sziranyi, T.; and Saupe, D. 2020. KonIQ-10k: An ecologically valid database for deep learning of blind image quality assessment. *IEEE Transactions on Image Processing*, 29: 4041–4056.
- Jia, M.; Tang, L.; Chen, B.-C.; Cardie, C.; Belongie, S.; Hariharan, B.; and Lim, S.-N. 2022. Visual prompt tuning. In *European Conference on Computer Vision*, 709–727. Springer.
- Jinjin, G.; Haoming, C.; Haoyu, C.; Xiaoxing, Y.; Ren, J. S.; and Chao, D. 2020. Pipal: a large-scale image quality assessment dataset for perceptual image restoration. In *Computer Vision—ECCV 2020: 16th European Conference, Glasgow, UK, August 23–28, 2020, Proceedings, Part XI 16*, 633–651. Springer.
- Ke, J.; Wang, Q.; Wang, Y.; Milanfar, P.; and Yang, F. 2021. Musiq: Multi-scale image quality transformer. In *Proceedings of the IEEE/CVF International Conference on Computer Vision*, 5148–5157.
- Khattak, M. U.; Rasheed, H.; Maaz, M.; Khan, S.; and Khan, F. S. 2023a. Maple: Multi-modal prompt learning. In *Proceedings of the IEEE/CVF Conference on Computer Vision and Pattern Recognition*, 19113–19122.
- Khattak, M. U.; Wasim, S. T.; Naseer, M.; Khan, S.; Yang, M.-H.; and Khan, F. S. 2023b. Self-regulating prompts: Foundational model adaptation without forgetting. In *Proceedings of the IEEE/CVF International Conference on Computer Vision*, 15190–15200.

- Kingma, D. P.; and Ba, J. 2014. Adam: A method for stochastic optimization. *arXiv preprint arXiv:1412.6980*.
- Larson, E. C.; and Chandler, D. M. 2010. Most apparent distortion: full-reference image quality assessment and the role of strategy. *Journal of electronic imaging*, 19(1): 011006.
- Li, C.; Zhang, Z.; Wu, H.; Sun, W.; Min, X.; Liu, X.; Zhai, G.; and Lin, W. 2023a. Agiqa-3k: An open database for ai-generated image quality assessment. *IEEE Transactions on Circuits and Systems for Video Technology*.
- Li, J.; Gao, M.; Wei, L.; Tang, S.; Zhang, W.; Li, M.; Ji, W.; Tian, Q.; Chua, T.-S.; and Zhuang, Y. 2023b. Gradient-regulated meta-prompt learning for generalizable vision-language models. In *Proceedings of the IEEE/CVF International Conference on Computer Vision*, 2551–2562.
- Li, X.; Gao, T.; Hu, R.; Zhang, Y.; Zhang, S.; Zheng, X.; Zheng, J.; Shen, Y.; Li, K.; Liu, Y.; et al. 2024. Adaptive Feature Selection for No-Reference Image Quality Assessment by Mitigating Semantic Noise Sensitivity. In *Forty-first International Conference on Machine Learning*. PMLR.
- Lin, H.; Hosu, V.; and Saupe, D. 2019. KADID-10k: A large-scale artificially distorted IQA database. In *2019 Eleventh International Conference on Quality of Multimedia Experience (QoMEX)*, 1–3. IEEE.
- Loshchilov, I.; and Hutter, F. 2019. Decoupled Weight Decay Regularization. In *International Conference on Learning Representations*.
- Ma, K.; Duanmu, Z.; Wu, Q.; Wang, Z.; Yong, H.; Li, H.; and Zhang, L. 2016a. Waterloo exploration database: New challenges for image quality assessment models. *IEEE Transactions on Image Processing*, 26(2): 1004–1016.
- Ma, K.; Liu, X.; Fang, Y.; and Simoncelli, E. P. 2019. Blind image quality assessment by learning from multiple annotators. In *2019 IEEE international conference on image processing (ICIP)*, 2344–2348. IEEE.
- Ma, K.; Wu, Q.; Wang, Z.; Duanmu, Z.; Yong, H.; Li, H.; and Zhang, L. 2016b. Group mad competition—a new methodology to compare objective image quality models. In *Proceedings of the IEEE Conference on Computer Vision and Pattern Recognition*, 1664–1673.
- Madhusudana, P. C.; Birkbeck, N.; Wang, Y.; Adsumilli, B.; and Bovik, A. C. 2022. Image quality assessment using contrastive learning. *IEEE Transactions on Image Processing*, 31: 4149–4161.
- Ponomarenko, N.; Jin, L.; Ieremeiev, O.; Lukin, V.; Egiazarian, K.; Astola, J.; Vozel, B.; Chehdi, K.; Carli, M.; Battisti, F.; et al. 2015. Image database TID2013: Peculiarities, results and perspectives. *Signal processing: Image communication*, 30: 57–77.
- Qin, G.; Hu, R.; Liu, Y.; Zheng, X.; Liu, H.; Li, X.; and Zhang, Y. 2023. Data-Efficient Image Quality Assessment with Attention-Panel Decoder. In *Proceedings of the Thirty-Seventh AAAI Conference on Artificial Intelligence*.
- Radford, A.; Kim, J. W.; Hallacy, C.; Ramesh, A.; Goh, G.; Agarwal, S.; Sastry, G.; Askell, A.; Mishkin, P.; Clark, J.; et al. 2021. Learning transferable visual models from natural language supervision. In *International conference on machine learning*, 8748–8763. PMLR.
- Saha, A.; Mishra, S.; and Bovik, A. C. 2023. Re-IQA: Un-supervised Learning for Image Quality Assessment in the Wild. In *Proceedings of the IEEE/CVF Conference on Computer Vision and Pattern Recognition*, 5846–5855.
- Sheikh, H. R.; Sabir, M. F.; and Bovik, A. C. 2006. A statistical evaluation of recent full reference image quality assessment algorithms. *IEEE Transactions on image processing*, 15(11): 3440–3451.
- Song, T.; Li, L.; Cheng, D.; Chen, P.; and Wu, J. 2023. Active Learning-Based Sample Selection for Label-Efficient Blind Image Quality Assessment. *IEEE Transactions on Circuits and Systems for Video Technology*.
- Srinath, S.; Mitra, S.; Rao, S.; and Soundararajan, R. 2024. Learning Generalizable Perceptual Representations for Data-Efficient No-Reference Image Quality Assessment. In *Proceedings of the IEEE/CVF Winter Conference on Applications of Computer Vision*, 22–31.
- Su, S.; Yan, Q.; Zhu, Y.; Zhang, C.; Ge, X.; Sun, J.; and Zhang, Y. 2020. Blindly assess image quality in the wild guided by a self-adaptive hyper network. In *Proceedings of the IEEE/CVF Conference on Computer Vision and Pattern Recognition*, 3667–3676.
- Tu, Z.; Wang, Y.; Birkbeck, N.; Adsumilli, B.; and Bovik, A. C. 2021. UGC-VQA: Benchmarking blind video quality assessment for user generated content. *IEEE Transactions on Image Processing*, 30: 4449–4464.
- Vanschoren, J. 2018. Meta-learning: A survey. *arXiv preprint arXiv:1810.03548*.
- Vu, T.; Lester, B.; Constant, N.; Al-Rfou, R.; and Cer, D. 2021. Spot: Better frozen model adaptation through soft prompt transfer. *arXiv preprint arXiv:2110.07904*.
- Wang, J.; Chan, K. C.; and Loy, C. C. 2023. Exploring clip for assessing the look and feel of images. In *Proceedings of the AAAI Conference on Artificial Intelligence*, volume 37, 2555–2563.
- Wu, H.; and Shi, X. 2022. Adversarial soft prompt tuning for cross-domain sentiment analysis. In *Proceedings of the 60th Annual Meeting of the Association for Computational Linguistics (Volume 1: Long Papers)*, 2438–2447.
- Xu, K.; Liao, L.; Xiao, J.; Chen, C.; Wu, H.; Yan, Q.; and Lin, W. 2024. Boosting Image Quality Assessment through Efficient Transformer Adaptation with Local Feature Enhancement. In *Proceedings of the IEEE/CVF Conference on Computer Vision and Pattern Recognition*, 2662–2672.
- Yang, S.; Wu, T.; Shi, S.; Lao, S.; Gong, Y.; Cao, M.; Wang, J.; and Yang, Y. 2022. Maniqa: Multi-dimension attention network for no-reference image quality assessment. In *Proceedings of the IEEE/CVF Conference on Computer Vision and Pattern Recognition*, 1191–1200.
- Yao, H.; Zhang, R.; and Xu, C. 2023. Visual-language prompt tuning with knowledge-guided context optimization. In *Proceedings of the IEEE/CVF conference on computer vision and pattern recognition*, 6757–6767.
- Ying, Z.; Niu, H.; Gupta, P.; Mahajan, D.; Ghadiyaram, D.; and Bovik, A. 2020. From patches to pictures (PaQ-2-PiQ):

Mapping the perceptual space of picture quality. In *Proceedings of the IEEE/CVF Conference on Computer Vision and Pattern Recognition*, 3575–3585.

Zhang, J.; Wu, S.; Gao, L.; Shen, H. T.; and Song, J. 2024. Dept: Decoupled prompt tuning. In *Proceedings of the IEEE/CVF Conference on Computer Vision and Pattern Recognition*, 12924–12933.

Zhang, W.; Ma, K.; Yan, J.; Deng, D.; and Wang, Z. 2018. Blind image quality assessment using a deep bilinear convolutional neural network. *IEEE Transactions on Circuits and Systems for Video Technology*, 30(1): 36–47.

Zhang, W.; Zhai, G.; Wei, Y.; Yang, X.; and Ma, K. 2023. Blind image quality assessment via vision-language correspondence: A multitask learning perspective. In *Proceedings of the IEEE/CVF Conference on Computer Vision and Pattern Recognition*, 14071–14081.

Zhao, K.; Yuan, K.; Sun, M.; Li, M.; and Wen, X. 2023. Quality-aware pre-trained models for blind image quality assessment. In *Proceedings of the IEEE/CVF Conference on Computer Vision and Pattern Recognition*, 22302–22313.

Zhou, K.; Yang, J.; Loy, C. C.; and Liu, Z. 2022a. Conditional prompt learning for vision-language models. In *Proceedings of the IEEE/CVF conference on computer vision and pattern recognition*, 16816–16825.

Zhou, K.; Yang, J.; Loy, C. C.; and Liu, Z. 2022b. Learning to prompt for vision-language models. *International Journal of Computer Vision*, 130(9): 2337–2348.

Zhu, B.; Niu, Y.; Han, Y.; Wu, Y.; and Zhang, H. 2023. Prompt-aligned gradient for prompt tuning. In *Proceedings of the IEEE/CVF International Conference on Computer Vision*, 15659–15669.

Zhu, H.; Li, L.; Wu, J.; Dong, W.; and Shi, G. 2020. MetaQA: Deep meta-learning for no-reference image quality assessment. In *Proceedings of the IEEE/CVF Conference on Computer Vision and Pattern Recognition*, 14143–14152.